Dalton Transactions

Accepted Manuscript

ROYAL SOCIETY OF CHEMISTRY

www.rsc.org/dalton

TOC

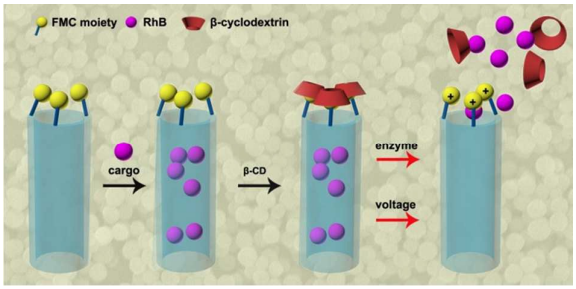

This work demonstrated that the development of a novel controlled release system which is sensitive to enzyme and voltage stimulus based on the mesoporous silica nanoparticles functionalized by ferrocene moiety and β-cyclodextrin as the nanovalves.

Journal Name

RSCPublishing

ARTICLE

Enzyme and voltage stimuli-responsive controlled release system based on β-cyclodextrin-capped mesoporous silica nanoparticles

Cite this: DOI: 10.1039/x0xx00000x

Received ooth January 2012,
Accepted ooth January 2012

DOI: 10.1039/x0xx00000x

www.rsc.org/

Yu Xiao, Tao Wang, Yu Cao, Xue Wang, Ye Zhang, Yunling Liu and Qisheng Huo*

Enzyme and voltage stimuli are more biological compatibility in the field of stimuli-responsive system and the release system based on β-cyclodextrin (CD) and ferrocene (Fc) has attracted much attention. Herein, mesoporous silica nanoparticles (MSNs) have been functionalized with the ferrocenyl moiety (Fc) which interacts with β-cyclodextrin (β-CD) to form an inclusion complex on the opening of the pores. The size effect of the inclusion complex makes the barriers on the opening of the pores. Based on these characteristics, the MSNs with nanovalves have been developed to be a release system. The release system shows a clear response to Heme protein (horseradish peroxidase or hemoglobin) and H_2O_2, glucose oxidase (GOD) with horseradish peroxidase (HRP) and glucose, or +1.5 V voltage based on the oxidation stimulus mechanism. Modulating the amount of enzyme or the discretion of the voltage makes the release system achieve a controlled one.

Introduction

Advanced nanoscale systems for drug delivery have recently received tremendous attention.[1] Stimuli-responsive controlled release systems releasing their cargo in the presence of specific stimulus are attractive for biomedicine application.[2, 3] Nanoscale stimuli-responsive release may be sensitive to specific stimulus, such as enzymes,[4, 5] electric fields,[6] temperature,[7] magnetic fields,[6, 8] ultrasounds,[9] near-infrared light,[10] pH,[11] and redox potential.[12] Because most processes in living organisms are ultimately controlled by enzymes, enzymes are increasingly used as triggers to change the properties of artificial materials to create the controlled release. The main strength of enzyme stimulus system compared to other stimuli clearly lies in their ability to interact with a biological environment with the same communication mechanism used by nature.[13] Weak electric fields can be used to achieve pulsed or sustained drug release through a variety of actuation mechanism, such as electrochemical reduction-oxidation and electric-field-driven movement of charged molecules.[1, 6] Artificial voltage-responsive release systems are well-suited to drug encapsulation and controlled release, and electrical stimulation is easy to realize in cells and the human body.[14] Multistimuli-responsive systems, which can achieve more functionalities and be modulated through more parameters, may present promising possibilities.[15]

Owing to impressive progress in material science and pharmaceutics, a broad range of nanocarriers with diverse sizes, architectures and surface properties have been designed.[1] These materials include liposomes,[16] polymer nanoparticles,[17] micelles,[18] dendrimers,[19] and inorganic nanoparticles[20] made of iron oxide, quantum dots, and gold or metal oxide frameworks. The size of these carriers is typically small to allow systemic or local administration, and to promote their diffusion within the cell.[21] MSNs have been extensively investigated as the carriers for applications in controlled release due to their adjustable particle size, large surface area, pore volume and high chemical and thermal stability.[22] The easily surface functionalization of MSNs makes them particularly attractive for establishment of release system based on various stimulus-response mechanisms.[23] All these unparalleled features make MSNs distinctive from other nanomaterials, lighting up a bright future in their biological applications. Tamanoi *et al.* reported that mesoporous silica nanoparticles can deliver the water-insoluble drug camptothecin into human pancreatic cancer cells.[24] Zink *et al.* reported that the functionalization of MSNs with molecules, polymeric moieties or supramolecular assemblies providing the material with great versatility while performing drug delivery

tasks.[25] Stoddart *et al* demonstrated the operation of molecular and supramolecular valves based on the MSNs in biologically relevant contexts using enzyme,[26] competitive binding,[27] pH,[28] redox[29] and light[30] as actuators.

So far, the host-guest interaction between β-cyclodextrin (CD) and ferrocenyl moiety (Fc) has been used to construct environmental sensitive systems[31, 32] based on the different stimuli, such as voltage[33], temperature and glucose.[34] Yuan *et al*. reported the voltage-responsive vesicles based on terminal host-guest interactions between polymer PS-β-CD and PEO-Fc.[14] Tan *et al*. reported that Alg-β-CD-F127-Fc (Alg-β-CD 3%, F127-Fc 22%) could form gel at 21℃ and entrap GOD in it.[35] The addition of glucose could induce the gel-sol transition. Rica *et al*. reported the ultrasensitive HRP sensor based on the interaction between Fc and β-CD.[36] Developing a new and suitable multi-sensitive system responded on above stimulus mechanisms based on MSNs is innovative.

Herein, we develop a novel controlled-release system that is successfully sensitive to enzyme or voltage stimuli. MSNs with hexagonally arranged pores are functionalized with ferrocene derivative groups. Mesoporous silica nanoparticles are not only the support of response, but also the container for guest molecules. The inclusion complex which is formed of ferrocenyl moiety and β-CD by the interaction between them effectively prevented the premature cargo release before stimulation. After stimulated by Heme protein (horseradish peroxidase or hemoglobin) and H_2O_2, glucose oxidase (GOD) with horseradish peroxidase (HRP) and glucose or +1.5 V voltage, the charged ferrocenyl moieties dissociated rapidly from the cavity. The β-CD leaves from the functionalized MSNs, which makes the nanovalves open and the cargo release.

Experimental

Chemicals and reagents

Horseradish peroxidase (HRP) and glucose oxidase (GOD) were purchased from Roche. Hydrogen peroxide (30%), Rhodamine B (RhB), glucose and ferrocenemonocarboxylic acid (FMC) were purchased from Sinopharm. Tetraethoxysilane (TEOS), β-cyclodextrin, 3-aminopropyltriethoxysilane (APTES), hemoglobin (Hb) N-(3-dimethylaminopropyl)-N ' -ethylcarbodiimidhydrochlorid (EDC) and N-hydroxysuccinimide (NHS) were purchased from Sigma-Aldrich. Cetyltrimethylammonium bromide (CTAB) was obtained from Huishi Biochemical Reagent Company of China.

Synthesis of MSNs and modification of MSNs with 3-aminopropyltriethoxysilane (NH_2-MSNs)

In the typical synthesis,[37] 0.5 g of CTAB, 1.75 mL of 2 M NaOH solution, 240 mL of H_2O were mixed and stirred at 80°C for a while. Then 2.5 mL of TEOS was added dropwise into the aqueous solution. The mixture solution gradually turned white and they were maintained at 80°C for another 2 h. The as-prepared MSNs were collected through centrifugation at 8000 rpm for 5 min. In order to remove the template, the surfactant extraction was performed by stirring the materials in 100 mL of ethanol with HCl at reflux for 12 h. Finally, the product was dried under vacuum overnight. As shown in Scheme 1, organic modification of MSN with 3-aminopropyltriethoxysilane (APTES) was performed by stirring 60 mg of MSNs with 108 mg of APTES in dry ethanol and refluxed for 24 h under nitrogen atmosphere.[38] The resulting white powder NH_2-MSNs was centrifuged and washed with ethanol.

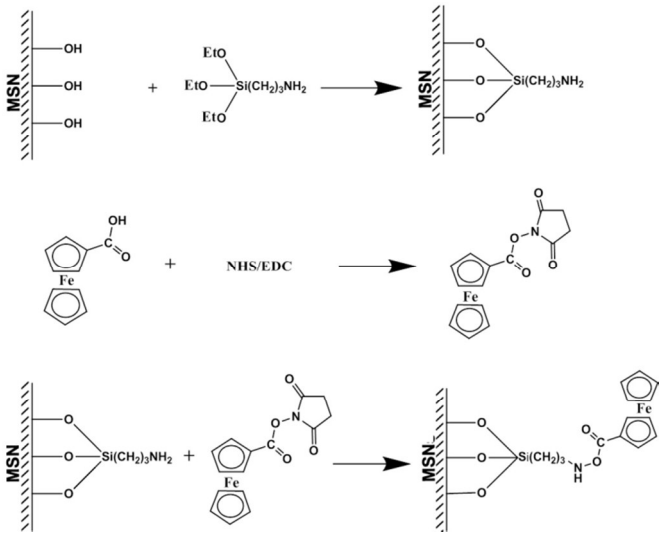

Scheme 1 Synthetic route of the FMC-MSNs.

Functionalization of NH_2-MSNs with FMC (FMC-MSNs)

FMC-MSNs were synthesis through carbodiimide coupling, as shown in Scheme 1. In brief,[39] 60 mg of FMC was dissolved thoroughly in 10 mL of 0.1 M pH 7.4 phosphate buffered saline (PBS). 300 mg of EDC and 250 mg of NHS were dissolved in the solution follow with continuous stirring for 45 min. The solution of 60 mg NH_2-MSNs dispersed in 1 mL of 0.1 M pH 7.4 PBS was added dropwise to the mixture under stirring at a low stirring rate for 24 h at room temperature. Then the produced conjugate was centrifuged and washed with the deionized water for several times. Finally, the obtained conjugate was dialyzed in a dialysis bag (cutoff: 3500) against deionized water at room temperature for 24 h by changing the water every 6 h to remove nonconjugated FMC.

RhB loading and β-cyclodextrin capping

30 mg of suspended FMC-MSNs was added into a solution of 5mM RhB in 12 mL of mixture DMF and H_2O (volume ratio = 1) for 16 h under stirring at room temperature. Then 85 mg of β-cyclodextrin was added into the mixture. After 24 h, the product was centrifuged and washed with the deionized water for several times. Then sample was dialyzed in a dialysis bag (cutoff: 3,500) against 1 L of pH 7.4 PBS for 4 h by changing the buffer solution every 1 h to remove the RhB molecules on

the surface of nanoparticles. The dialysis was terminated until the water outside the dialysis bag exhibited negligible RhB fluorescence.

Controlled release experiment

The RhB-loading and β-cyclodextrin-capping MSNs (2 mg) were suspended in PBS then putted into dialysis bag (cutoff: 3500), which was immersed into the beaker which was stirred gently with 25 mL of PBS containing a certain concentration of hydrogen peroxide or glucose. To activate the nanovalves was started by adding enzyme. During this period time, fluorescence spectrums of the solution were recorded at predetermined times. The amount of released RhB was quantified by plotting the fluorescence intensity of RhB as a function of time.

The RhB-loading functionalized MSNs were suspended in the buffer solution. After limited premature release, the system was exerted different voltages (+ 0.5 V or + 1.5 V) according to literature.[14] The experimental setup was shown in Fig. S1. The amount of released RhB was quantified according to the above methods.

Characterization

Powder X-ray diffraction data were collected on a SIEMENS D5005 diffractometer. The morphologies and dimension of the samples were determined by using a JEOL JSM-6700F field emission scanning electron microscope and by a JEOL JEM-3010 transmission electron microscope (TEM). The adsorption-desorption isotherms of nitrogen were measured at 77K using a micromeritics ASAP 2420 analyzer and the pore size distributions were calculated from the adsorption branches of the isotherms on the basis of the BJH model The sample was degassed at 120°C for at least 10 h before measurement. Elemental analysis was performed on a Perkin-Elmer 2400 Series II CHNS/O elemental analyzer. The successful functionalization of MSNs was validated using the inductively coupled plasma analyses, which were carried out on a Perkin-Elmer Optima 3300DV ICP instrument. The samples were dissolve in the aqueous solution of HF (10 wt.%). Release of RhB from the mesoporous of the MSNs was monitored by using an Edinburgh Instruments FLS920 spectrofluorimeter equipped with both continuous (450 W) and pulsed xenon lamps. The voltage stimuli were obtained from the CHI660C from CHI Instruments.

Results and discussion

Synthesis, characterization and functionalization of MSNs

In this study, we synthesize the MSNs with hexagonally arranged pores. MSNs are modified with APTES into NH_2-MSNs through grafting. After functionalization of NH_2-MSNs with FMC, we establish a dual stimuli-responsive cargo release system through the nanovalves based on the host-guest interaction between FMC-MSNs and β-CD.

The morphology of MSNs and functionalized MSNs has been studied by scanning electron microscopy (SEM). Fig. 1 shows the SEM images of MSNs and NH_2-MSNs. Both MSNs and NH_2-MSNs are well homo-generous and mono-dispersed spherical nanoparticles with an average size of ca. 100nm. The shape and size of the particles are retained after the modification of MSNs with APTES.

The zeta potential (listed in Table 1) for MSNs is -33.0 mV. Due to the introduction of positively charged amino group after modification, the zeta potential changes to +21.9 mV. The nitrogen content in the NH_2-MSNs is 2.88% based on the CHN elemental analysis results, which is clearly higher than that in the MSNs (0.10%). These results confirmed that the modification of MSNs with APTES is successful.

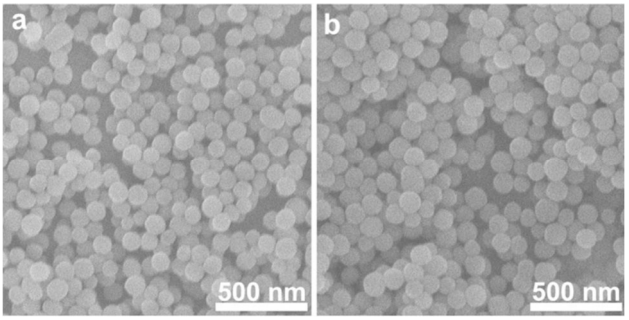

Fig. 1 SEM images of the (a) MSN, (b) NH_2-MSNs.

Table 1 Considerable properties of MSNs and functionalized MSNs

Samples	Zeta Potential in pH 6.8 solution /mV[a]	Nitrogen wt.%[b]	Iron element wt.%[c]
MSNs	-33.0	0.10	--
NH_2-MSNs	+21.9	2.88	--
FMC-MSNs	-15.8	2.64	7.0

[a] The measurement solution is deionized water.
[b] The measurement method is the CHN elemental analysis.
[c] The measurement method is the inductively coupled plasma (ICP) analysis.

The pore structures of MSNs and functionalized MSNs have been studied by transmission electron microscopy (TEM) (shown in Fig. 2). TEM images reveal the ordered 2D hexagonal arrays of cylindrical pores of MSNs and NH_2-MSNs. The TEM image of FMC-MSNs shows the mesostructure still exists without obvious difference. The pore structure of RhB-loading and β-CD-capping FMC-MSNs can not be observed clearly after cargo loading and β-CD capping, which result from the RhB contained in the pores and the β-CD capping on the opening of the pores leading to a lower image contrast between the channel and silica wall.

The inductively coupled plasma (ICP) analysis result listed in Table 1 shows the mass percentage of iron element in the FMC-MSNs is 7%. In addition, the zeta potential changes from +21.9 mV to -15.8 mV after the functionalization of NH_2-MSNs with FMC. These results confirm that FMC has successfully been bonded to NH_2-MSNs.

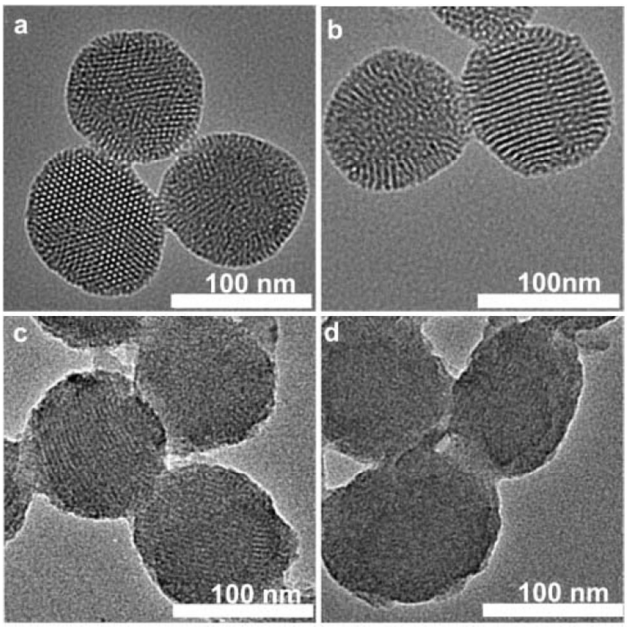

Fig. 2 TEM images of (a) MSNs, (b) NH_2-MSNs, (c) FMC-MSNs, (d) RhB-loading and β-CD-capping FMC-MSNs.

This feature was further confirmed by the small-angle powder X-ray diffraction (XRD) patterns in Fig. 3. For MSNs and NH_2-MSNs, four diffraction peaks are observed and indexed as (100), (110), (200), and (210) planes with p6mm symmetry, indicating atypical two dimensional hexagonal mesostructure.[40] The intensities of XRD peaks of FMC-MSNs and RhB-loading and β-CD-capping FMC-MSNs decrease and the width of that broaden due to the functionalization of FMC, cargo loading and β-CD capping.

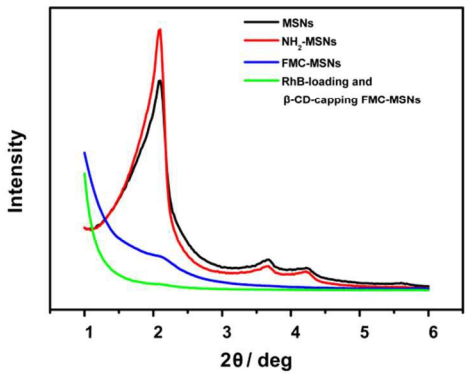

Fig. 3 Small-angle powder X-ray diffraction (XRD) patterns of MSNs (black), NH_2-MSNs (red), FMC-MSNs (blue) and RhB-loading, β-CD-capping FMC-MSNs (green).

Moreover, the porous properties of MSNs and functionalized MSNs were measured by nitrogen adsorption-desorption isotherms in Fig. 4. The type IV adsorption isotherms of MSNs, NH_2-MSNs and FMC-MSNs confirmed the cylindrical pore structure as it can be seen in the TEM images.[41] The change of the adsorption isotherm of RhB-loading and β-CD-capping FMC-MSNs are due to RhB loading and β-CD capping. Table 2 lists the porous properties of samples. The BET surface area of MSNs is 993 m^2 g^{-1}. As expected, the surface areas of NH_2-MSNs and FMC-MSNs compared to MSNs decrease considerably and the surface areas of RhB-loading and β-CD-capping FMC-MSNs further decreases. The pore volumes and pore diameters of MSNs decrease respectively after modification, functionalization, RhB loading and β-CD capping.

In conclusion, we successfully develop nanocarriers using the FMC functionalized MSNs. The nanocarriers supply the foundation of the study on the dual stimuli-responsive controlled drug release.

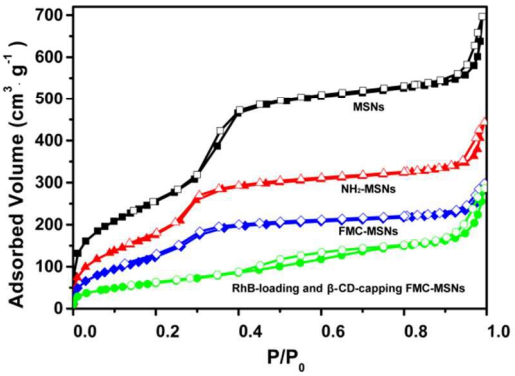

Fig. 4 The nitrogen adsorption-desorption isotherms of MSNs (black), NH_2-MSNs (red), FMC-MSNs (blue) and RhB-loading, β-CD-capping FMC-MSNs (green).

Table 2 Porous properties of MSNs and functionalized MSNs[a]

Samples	S_{BET}/m^2 g^{-1}	V_p/cm^3 g^{-1}	d_p/nm
MSNs	993	0.90	3.1
NH_2-MSNs	699	0.52	2.6
FMC-MSNs	513	0.35	2.5
RhB-loading and β-CD-capping FMC-MSNs	228	0.19	--

[a] S_{BET}, BET surface area; V_p, pore volume at P/P_0 0.92; d_p, pore diameter calculated from BJH improved KJS method.

Enzyme-responsive controlled release of cargo

This cargo release system is depended on the nanovalves based on the inclusion complex formed by β-CD with ferrocenyl moiety through the noncovalent host-guest interaction. When β-CDs interact with the ferrocene (Fc) groups which have been modified onto the pore orifices of MSNs, the inclusion complexes become caps to prevent the cargo release. Normally, uncharged Fc species or its derivatives are strongly bonded in the hydrophobic cavity of β-CD, whereas the charged species (Fc^+) dissociate rapidly from the cavity (shown in Scheme 2).[42, 43] It is the key factor for the controlled release system to change the strength of host guest interaction by oxidation of ferrocenyl moieties.

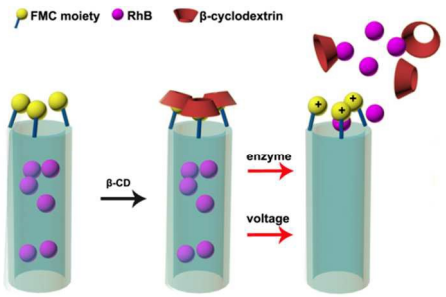

Scheme 2 The schematic diagram of the release of RhB from the functionalized MSNs.

The release system firstly is employed as an enzyme-responsive model to study the cargo release property. In the enzyme-responsive model, there are two oxidation pathways. The first pathway is that Fc can be oxidized to Fc^+ when the present of H_2O_2 and Heme protein as enzyme catalysts.[36] The other one is the oxidation of Fc without H_2O_2 when the present of HRP, GOD and glucose.[44]

For the first oxidation mechanism, Fig. 5 shows the release of RhB from RhB-loading and β-CD-capping FMC-MSNs upon Heme proteins stimuli. The bottom line in Fig. 5 shows that there is a limited premature release without stimuli. When adding HRP and Hb in the system, the rates of cargo release are faster and at the same point in time the amount of cargo release are higher. Due to the different enzyme catalytic abilities, the cargo release properties are different upon HRP and Hb stimuli. It is noteworthy that the amount of cargo release raises upon the more Heme proteins content stimuli in the system. The results indicate that the enzyme responsive model achieves an enzyme-responsive controlled release system.

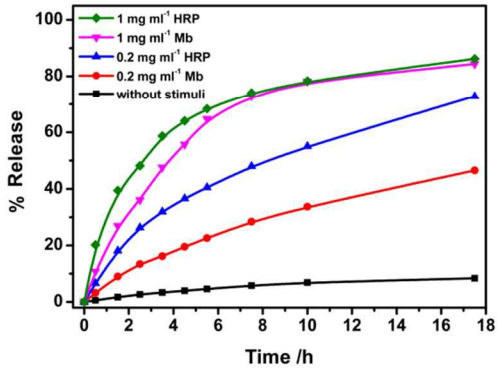

Fig. 5 Controlled releases of RhB from RhB-loading and β-CD-capping FMC-MSNs upon different content Heme protein stimuli in the presence of 50 mM H_2O_2 in comparison with the free release of RhB without stimuli.

HRP and Hb are the members of Heme proteins family which have significant transmission electron, delivering oxygen and physiological activity of enzyme action.[45] However, HRP is a kind of peroxidase and it can easily combine with hydrogen peroxide. This makes the valence of iron element change and promotes the oxydic reaction at the same time.[36] On the other hand, Hb combines with oxygen and its main function is the delivering oxygen. Although Hb has certain ability of oxidation, this ability of Hb is weaker than which of HRP under the same concentration. Hence, the amount of release is higher especially upon less HRP stimuli than upon less Hb stimuli at the same point in time. In conclusion, the controlled release system works when adding the Heme proteins as stimuli.

For the second oxidation mechanism without H_2O_2, the significant step for this mechanism is producing H_2O_2 through oxidation of glucose by GOD.

As shown in Fig. 6, the controlled release of cargo has been achieved through modulation of GOD stimuli levels. Because GOD can oxidize glucose to produce hydrogen peroxide, the generation of hydrogen peroxide is immediately reduced by HRP. The HRP becomes the oxidation state of HRP. The oxidation state of HRP continues oxidizing Fc to Fc^+. Then the oxidation state of HRP becomes the HRP with the ability of reduction.[35] Hence, the Fc becomes Fc^+ in cycles. The β-CD dissociates rapidly from FMC^+-MSNs and the controlled release works.

Because the two enzymic catalytic reactions happen continuously, the enzyme and glucose sensitive controlled release needs long time to reach the maximum amount of release. The fact reflects on the release profiles is that the amount of release is lower upon enzyme and glucose stimuli than upon Heme proteins stimuli at the same point in time. Nevertheless, the oxidant hydrogen peroxide still oxidizes a certain amount of Fc to Fc^+.[46] Fig. S1 shows a limited release with the addition of GOD with glucose comparing to that of GOD with HRP and glucose.

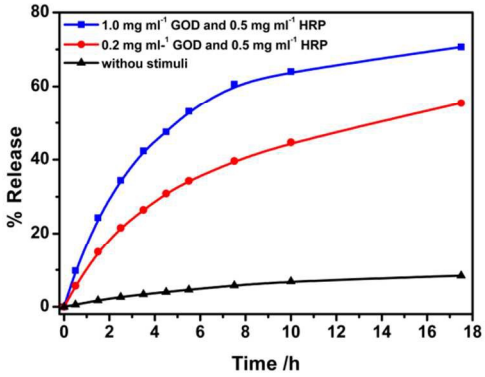

Fig. 6 Controlled release of RhB from RhB-loading and β-CD-capping FMC-MSNs upon different content GOD in presence of 10 mM glucose and 0.5 mg ml^{-1} HRP.

Voltage-responsive controlled release of cargo

The artificial voltage-responsive system is well-suited to drug delivery and the controlled release, and electrical stimulation is easy to realize the cells and the human body.[1] The key of the voltage stimuli also is the oxidation of Fc to Fc^+. The charged species (Fc^+) dissociate rapidly from the cavity, and this process can be reversibly switched under external voltage.[47, 48] The stander electrode potential of Fc^+/Fc ($E^0_{Fc^+/Fc}$) is +0.32 V. Upon

the higher voltage than +0.32 V can trigger the release system works.[49, 50] Fig. 7 shows the controlled release of RhB from the functional MNSs upon different voltage stimuli after limited premature release. From the curves in Fig. 7, an obvious release is observed upon application of high voltage (+1.5 V). And RhB molecules show a slower release upon lower voltage stimuli (+0.5 V).

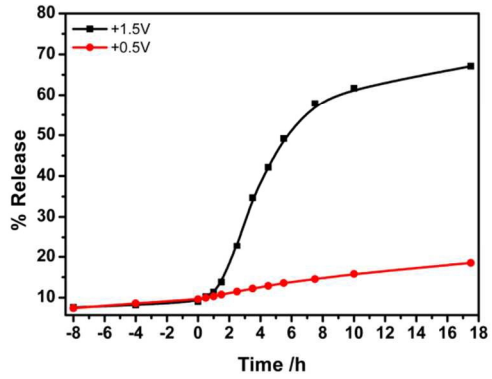

Fig. 7 Controlled release of RhB from RhB-loading and β-CD-capping FMC-MSNs upon different voltage stimuli.

Upon +1.5 V voltage stimuli, FMC-MSNs are oxidized into charged FMC^{+}-MSNs.[33] Then the controlled release works as how the enzyme-responsive release works. Exerting a voltage of +0.5 V or +1.5 V can activate the controlled release and the release performances upon the different voltage stimuli are different.[14]

Conclusions

We successfully develop the controlled release system through the host-guest interaction between β-CD and FMC-MSNs. The release system shows response to Heme protein based on two oxidation pathways, adding the H_2O_2 into the system and producing H_2O_2 through oxidation of glucose by GOD in the system. Due to the unique characteristic of ferrocenyl moiety, the release is sensitive to +1.5 V voltage. Response to multi-stimulus can even further improve drug delivery. The controlled release system in response to enzyme with glucose and voltage has the unique potential in application in both sensing changes in blood glucose levels and electrochemical therapeutics.

Acknowledgements

This work was supported by the National Natural Science Foundation of China (No. 21371067, 21373095 and 21171064).

Notes and references

State Key Laboratory of Inorganic Synthesis and Preparative Chemistry, College of Chemistry, Jilin University, Changchun, China. Fax: 0086-431-85168602; Tel: +86-431-85168602; E-mail: huoqisheng@jlu.edu.cn

† Electronic Supplementary Information (ESI) available: the experimental setup for the release upon different voltages, the release profiles by adding GOD and glucose comparing to that of GOD, HRP and glucose. See DOI: 10.1039/b000000x/

1. S. Mura, J. Nicolas and P. Couvreur, *Nat Mater*, 2013, **12**, 991-1003.
2. S. A. Abouelmagd, H. Hyun and Y. Yeo, *Expert Opin. Drug Del.*, 2014, **11**, 1601-1618.
3. F. Puoci, G. Cirillo, M. Curcio, O. I. Parisi, F. Iemma and N. Picci, *Expert Opin. Drug Del.*, 2011, **8**, 1379-1393.
4. M.-H. Xiong, Y. Bao, X.-Z. Yang, Y.-C. Wang, B. Sun and J. Wang, *J. Am. Chem. Soc.*, 2012, **134**, 4355-4362.
5. G. L. Zhang, M. L. Yang, D. Q. Cai, K. Zheng, X. Zhang, L. F. Wu and Z. Y. Wu, *Acs Appl. Mater. Interfaces*, 2014, **6**, 8042-8047.
6. J. Ge, E. Neofytou, T. J. Cahill, R. E. Beygui and R. N. Zare, *ACS Nano*, 2011, **6**, 227-233.
7. Z. S. Al-Ahmady, W. T. Al-Jamal, J. V. Bossche, T. T. Bui, A. F. Drake, A. J. Mason and K. Kostarelos, *ACS Nano*, 2012, **6**, 9335-9346.
8. E. Ruiz-Hernández, A. Baeza and M. Vallet-Regí, *ACS Nano*, 2011, **5**, 1259-1266.
9. A. Ranjan, G. C. Jacobs, D. L. Woods, A. H. Negussie, A. Partanen, P. S. Yarmolenko, C. E. Gacchina, K. V. Sharma, V. Frenkel, B. J. Wood and M. R. Dreher, *J. Controlled Release*, 2012, **158**, 487-494.
10. A. Schroeder, M. S. Goldberg, C. Kastrup, Y. Wang, S. Jiang, B. J. Joseph, C. G. Levins, S. T. Kannan, R. Langer and D. G. Anderson, *Nano Lett.*, 2012, **12**, 2685-2689.
11. E. Koren, A. Apte, A. Jani and V. P. Torchilin, *J. Controlled Release*, 2012, **160**, 264-273.
12. Y. Sun, X. L. Yan, T. M. Yuan, J. Liang, Y. J. Fan, Z. W. Gu and X. D. Zhang, Biomaterials, 2010, 31, 7124-7131.
13. M. Zelzer, S. J. Todd, A. R. Hirst, T. O. McDonald and R. V. Ulijn, *Biomaterials Science*, 2013, **1**, 11-39.
14. Q. Yan, J. Yuan, Z. Cai, Y. Xin, Y. Kang and Y. Yin, *J. Am. Chem. Soc.*, 2010, **132**, 9268-9270.
15. J. Dong, Y. N. Wang, J. Zhang, X. W. Zhan, S. Q. Zhu, H. Yang and G. J. Wang, *Soft Matter*, 2013, **9**, 370-373.
16. K.-J. Chen, H.-F. Liang, H.-L. Chen, Y. Wang, P.-Y. Cheng, H.-L. Liu, Y. Xia and H.-W. Sung, *ACS Nano*, 2012, **7**, 438-446.
17. A. Maksimenko, D. T. Bui, D. Desmaele, P. Couvreur and J. Nicolas, *Chem. Mater.*, 2014, **26**, 3606-3609.
18. Q. Huo, J. Liu, L.-Q. Wang, Y. Jiang, T. N. Lambert and E. Fang, *J. Am. Chem. Soc.*, 2006, **128**, 6447-6453.
19. H. M. Meng, X. B. Zhang, Y. F. Lv, Z. L. Zhao, N. N. Wang, T. Fu, H. H. Fan, H. Liang, L. P. Qiu, G. Z. Zhu and W. H. Tan, *Acs Nano*, 2014, **8**, 6171-6181.
20. J. Hu, G. Zhang and S. Liu, *Chem. Soc. Rev.*, 2012, **41**, 5933-5949.
21. R. de la Rica, D. Aili and M. M. Stevens, *Advanced Drug Delivery Reviews*, 2012, **64**, 967-978.
22. Slowing, II, J. L. Vivero-Escoto, C. W. Wu and V. S. Y. Lin, *Advanced Drug Delivery Reviews*, 2008, **60**, 1278-1288.
23. C. Coll, A. Bernardos, R. Martínez-Máñez and F. Sancenón, *Acc. Chem. Res.*, 2012, **46**, 339-349.
24. J. Lu, M. Liong, J. I. Zink and F. Tamanoi, *Small*, 2007, **3**, 1341-1346.

25. Z. Li, J. C. Barnes, A. Bosoy, J. F. Stoddart and J. I. Zink, *Chem. Soc. Rev.*, 2012, **41**, 2590-2605.
26. K. Patel, S. Angelos, W. R. Dichtel, A. Coskun, Y.-W. Yang, J. I. Zink and J. F. Stoddart, *J. Am. Chem. Soc.*, 2008, **130**, 2382-2383.
27. K. C. F. Leung, T. D. Nguyen, J. F. Stoddart and J. I. Zink, *Chem. Mater.*, 2006, **18**, 5919-5928.
28. O. S. Miljanic, W. R. Dichtel, S. Mortezaei and J. F. Stoddart, *Org. Lett.*, 2006, **8**, 4835-4838.
29. R. Hernandez, H. R. Tseng, J. W. Wong, J. F. Stoddart and J. I. Zink, *J. Am. Chem. Soc.*, 2004, **126**, 3370-3371.
30. T. D. Nguyen, Y. Liu, S. Saha, K. C. F. Leung, J. F. Stoddart and J. I. Zink, *J. Am. Chem. Soc.*, 2007, **129**, 626-634.
31. A. Harada, Y. Takashima and M. Nakahata, *Acc. Chem. Res.*, 2014, **47**, 2128-2140.
32. R. L. Sun, L. Wang, H. J. Yu, A. Zain ul, Y. S. Chen, J. Huang and R. B. Tong, *Organometallics*, 2014, **33**, 4560-4573.
33. L. Peng, A. C. Feng, H. J. Zhang, H. Wang, C. M. Jian, B. W. Liu, W. P. Gao and J. Y. Yuan, *Polymer Chemistry*, 2014, **5**, 1751-1759.
34. Z. Q. Dong, Y. Cao, Q. J. Yuan, Y. F. Wang, J. H. Li, B. J. Li and S. Zhang, *Macromol. Rapid Commun.*, 2013, **34**, 867-872.
35. L. Tan, Y. Liu, W. Ha, L.-S. Ding, S.-L. Peng, S. Zhang and B.-J. Li, *Soft Matter*, 2012, **8**, 5746-5749.
36. R. de laRica, R. M. Fratila, A. Szarpak, J. Huskens and A. H. Velders, *Angew. Chem. Int. Ed.*, 2011, **50**, 5704-5707.
37. L. Xing, H. Zheng, Y. Cao and S. Che, *Adv. Mater.*, 2012, **24**, 6433-6437.
38. D. H. Tang, L. Zhang, Y. L. Zhang, Z. A. Qiao, Y. L. Liu and Q. S. Huo, *J. Colloid Interface Sci.*, 2012, **369**, 338-343.
39. J.-D. Qiu, J. Guo, R.-P. Liang and M. Xiong, *Electroanalysis*, 2007, **19**, 2335-2341.
40. B. Guan, Y. Cui, Z. Ren, Z.-a. Qiao, L. Wang, Y. Liu and Q. Huo, *Nanoscale*, 2012, **4**, 6588-6596.
41. Y.-L. Sun, Y. Zhou, Q.-L. Li and Y.-W. Yang, *Chem. Commun.*, 2013, **49**, 9033-9035.
42. M. Nakahata, Y. Takashima and A. Harada, *Angew. Chem. Int. Ed.*, 2014, **53**, 3617-3621.
43. S. Angelos, E. Choi, F. Voegtle, L. De Cola and J. I. Zink, *Journal of Physical Chemistry C*, 2007, **111**, 6589-6592.
44. M. Ortiz, L. Wilson, M. L. Botero, P. Baker, E. Iwuoha, A. Fragoso and C. K. O'Sullivan, *Electroanalysis*, 2014, **26**, 1481-1487.
45. S. Hofbauer, I. Schaffner, P. G. Furtmuller and C. Obinger, *Biotechnology Journal*, 2014, **9**, 461-473.
46. K. Shang, X. Wang, B. Sun, Z. Cheng and S. Ai, *Biosens. Bioelectron.*, 2013, **45**, 40-45.
47. A. Harada, *Acc. Chem. Res.*, 2001, **34**, 456-464.
48. A. E. Kaifer, *Acc. Chem. Res.*, 1999, **32**, 62-71.
49. A. Samanta and B. J. Ravoo, *Chemistry – A European Journal*, 2014, **20**, 4966-4973.
50. A. Feng, Q. Yan, H. Zhang, L. Peng and J. Yuan, *Chem. Commun.*, 2014, **50**, 4740-4742.